Reports in Mechanical Engineering
Vol. 5, No. 1, 2024, pp. 68-81
ISSN: 2683-5894, DOI: https://doi.org/10.31181/rme413

Investigation of Material Nonlinearities in Surface Effects and Bulk on the Vibration Characteristics of Nanobeams

Nihayat Hussein Ameen
College of Agriculture, University of Kirkuk, Iraq.

Article Info

Article history:

Received May 29, 2024
Revised July 27, 2024
Accepted August 29, 2024

Keywords:

Materially Nonlinearities
Surface Effects
Vibration of Nanobeams

ABSTRACT

The surface effects play an important role in the vibrational properties of nanostructures. Investigating the nonlinear vibrations of nanobeams, the nonlinear material effects on surface effects have not been considered. This study aims to do research on the effect of material nonlinear coming from the stress-strain nonlinear equation on surface effects in order to increase the calculation accuracy. The effect of materially nonlinear behaviors of the bulk and surface effects in the presence of nonlinear *Von Kármán* strains are considered simultaneously. The governing equation based on the Hamilton principle and then the governing nonlinear differential equation based on applying the Galerkin's method have been extracted. The obtained nonlinear differential equation possesses cubic and quantic nonlinearities, which are due to the geometric and the materially nonlinear behaviors, respectively. The quantic nonlinearity is only due to the materially nonlinear behavior of bulk and surface effects. The temporal response and nonlinear frequency of nanobeams are obtained by solving the nonlinear differential equation based on the modified Lindstedt–Poincaré method. The results represent the simultaneous effects of the materially nonlinear behaviors of the bulk and surface layers on the temporal response and nonlinear frequency of the nanobeam. To examine the validity of the results, the obtained natural frequencies are compared with other studies in the absence of the materially nonlinear term.

Corresponding Author:

NIHAYAT HUSSEIN AMEEN
College of Agriculture, University of Kirkuk, Iraq
Email: mnas_int@uokirkuk.edu.iq

1. Introduction

Nowadays, nanotechnology has been turned to one of the most important fields in engineering science. Considering the applications of nanostructures in different devices, such as nano-resonators (Hamidi, Hosseini, Hassannejad, et al., 2020; Mahmoud, 2016) , recognizing gas atoms (Arash & Wang, 2013), devices' memories (Bunch et al., 2007), absorber systems (Qasim et al., 2018), and composite materials (Kakei et al., 2018; Kakei et al., 2019; Kuilla et al., 2010), many investigators developed passions to determine the mechanical behaviors of these structures in nanoscale. The effects of size are important in studying the vibrational behavior (Wang & Wang, 2011) of buckling (Nejad et al., 2016) and the failure (Zhao et al., 2012) of nanoscale structures. In order to prove the size-dependency, researchers have used the nonlocal and nonlocal strain gradient theories (Alizadeh Hamidi et al., 2020; Hamidi, Hosseini, Hayati, et al., 2020; Khosravi, Hosseini, & Hamidi, 2020; Khosravi, Hosseini, Hamidi, et al., 2020). Thus, Dang and Nguyen (Dang & Nguyen, 2021) carried out the buckling and nonlinear vibrations of a porous FG nanobeam. They utilized the Von Kármán strains to illustrate the nonlinear effects and obtained the governing equation with the help of nonlocal strain gradient. Moreover, they evaluated the effect of the power-law index and porosity in results. Manjur Alam et al. (Alam & Mishra, 2021) studied the nonlinear vibrational behavior of a FG nanobeam embedded in a nonlinear elastic medium. To show the nonlinearity effects, they established the Von Kármán strains in modeling nanobeams. Furthermore, they assessed the influences of the medium's shear interactions on the nanobeam's natural frequencies. Dang (Dang, 2020) carried out the nonlinear vibrations and buckling of a nanobeam based on the nonlocal strain

gradient theory. In their models, the nanobeam was under the axial compressive force. Furthermore, the critical buckling forces and the natural frequencies were calculated. Jazi (Jazi, 2020) investigated the forced nonlinear vibrations of a double Timoshenko nanobeam considering a concentrated moving force particle. The vibrational equations and the influence of velocity of particle's movement on the dynamic behavior of the nanobeam. Ebrahimi and Hosseini (Ebrahimi & Hosseini, 2021) evaluated the dynamic instability and nonlinear vibrations of the Euler-Bernoulli nanobeam. The desired nanobeam was under the thermo-magneto-mechanical loads. Also, the desired model was under the external parametric excitation. As a follow-up, to show the instability regions, the parametric excitation effect was investigated. Hieu et al. (Hieu & Bui, 2020), studied the nonlinear vibrations of a FG nanobeam employing the nonlocal strain gradient theory. Meanwhile, they used the Von Kármán strains to show the nonlinearity. Moreover, the thickness effect on the natural frequency was assessed. Ghadiri and Norouzi (Noroozi & Ghadiri, 2020) carried out the nonlinear forced vibrations of a nanobeam under an external axial excitation force. They considered the influence of gravity to derive the governing equations and examined the effect of attenuation on the dynamic stability of a nanobeam. Şimşek (Şimşek, 2014) illustrated nonlinear vibrations based on the nonlocal theory. The governing equations were obtained based on nonlinear Von Kármán strains. Eventually, the natural frequencies were utilized to analyze the boundary condition. Shafiei et al. (Shafiei et al., 2016) illustrated the nonlinear vibrations of the nanobeam based on nonlocal theory. The properties of the nanobeam were considered longitudinally. They solved the equations based on GDQ and obtained the natural frequencies. The effect of AFG (axially functionally graded) power-law index on the natural frequency was explained. Hasheminejad and Gheshlaghi (Gheshlaghi & Hasheminejad, 2011) studied the nonlinear vibrations of the nanobeam considering the surface effect. They applied the nonlocal theory to prove the size effect and analyzed the effect of nanobeam's thickness in the presence of surface effect on the natural frequency. Zhao et al. (Zhao et al., 2021) carried out the vibrational behavior of the Timoshenko nanobeam regarding the surface effect. They used molecular dynamics and generalized differential quadrature methods to understand the surface effects on the vibrations of nanobeam. Sourani et al. (Sourani et al., 2020) studied the dynamic stability of a Euler-Bernoulli nanobeam, considering the external longitudinal excitation force. In the desirable model, the surface effects had been considered. The governing equation was solved based on Bolotin and Incremental Harmonic Balance (IHB) methods and dynamic instability regions were examined for different parameters, such as the surface effect, longitudinal scale parameter, and temperature changes. Esfahani et al. (Esfahani et al., 2019) evaluated the nonlinear vibrations of FG nanobeams considering the surface effects based on nonlocal theory. They considered the Casimir forces on their governing equation, and in obtained results, they investigated the surface effects on the nanobeam's frequency response. The sources examined in the introduction section show the nonlinear vibrations of nanobeams only by considering geometric nonlinear Von Kármán strains. Meanwhile, in this case, in the study of nonlinear vibrations of nanobeams, in addition to geometric nonlinearity, the material nonlinearity is also considered. Also, due to the importance of surface effects on dynamic characteristics, for the first time, the materially nonlinear effect of bulk and surface layers are investigated, simultaneously. As a result, the governing equations are obtained using the Hamilton principle, taking into account material nonlinearity and surface effects. The governing equations are solved using the modified Lindstedt–Poincaré method. The natural frequency and responses obtained are examined for the material nonlinearity of the surface layers and bulk, and the compressive preload force. To show the accuracy of the results, the obtained natural frequency is compared with the results in the literature in the absence of material nonlinearity.

2. The Surface Elasticity Theory

To obtain the nonlinear vibration equation of the nanobeam, assuming that the nanobeam is only under pure bending (Rao, 2007), according to Euler-Bernoulli's theory, the displacement field for any desired point in x, y, and z directions is as follows:

$$u_x(x,z,t) = -z\frac{\partial w(x,t)}{\partial x}, u_y(x,z,t) = 0, u_z(x,z,t) = w(x,t) \quad (1)$$

Assuming Von Kármán nonlinear strains, the only non-zero strain component is expressed as follows:

$$\varepsilon_{xx} = \varepsilon_0 - z\varepsilon_1 = \frac{1}{2}\left(\frac{\partial w}{\partial x}\right)^2 - z\frac{\partial^2 w}{\partial x^2} \quad (2)$$

Considering Von Kármán nonlinear strains, the nonlinear strain stress equation for the nanobeam can be stated as follows (Lee et al., 2008):

$$\sigma_{xx} = \varepsilon_{xx}E + \varepsilon_{xx}^2 D \quad (3)$$

In Eq. (3), $D$is the third-order elastic modulus, which expresses the materially nonlinear behavior of the bulk, and E represents the Young's modulus. The surface effects on the mechanical behavior of nanomaterials are obtained by considering surface energy or surface stresses. The surface stress created in the nanobeam is as follows (Cammarata, 1994; C. Chen et al., 2006):

$$\sigma^s = \tau^0 + E_s\varepsilon_{xx} \tag{4}$$

Given that the surface stress in Eq. (4) is linear, according to Eq. (3), it can be considered nonlinear. In this case, Eq. (4) is written as follows:

$$\sigma^s = \tau^0 + E_s\varepsilon_{xx} + D^s\varepsilon_{xx}^2 \tag{5}$$

Eq. (5) shows the materially nonlinear behavior for the surface layers, and D^s, E_s and τ^0 show the surface effects on the vibrational equations and are defined in the form of the third-order surface modulus of elasticity, the surface elastic modulus, and the residual surface tension, respectively. Also, D^s stands for the materially nonlinear behavior of surface layers in this equation. According to the Young-Laplace equation (T. Chen et al., 2006; Gurtin et al., 1998), the $\langle\tau_{ij}^+ - \tau_{ij}^-\rangle n_i n_j$ stress, in a region of the surface, is defined as follows:

$$\langle\tau_{ij}^+ - \tau_{ij}^-\rangle n_i n_j = \tau^0\kappa \tag{6}$$

According to Eq. (6), κ represent the curvature of the surface, and $n_i$is the normal unit vector of the surface. Due to the fact that the curvature of the bending of the beam is approximated as:$w''(x)$, in the unreformed configuration, we will have $w''(x) = 0$. Therefore, the residual surface stress will not affect the structure. For the deformed beam, the residual surface tension creates a transverse force distributed in the longitudinal direction, which according to the Laplace-Young equation predicts the transverse force as follows (Wang & Feng, 2007, 2009):

$$q(x) = Hw''(x) \tag{7}$$

in which, H is equivalent to $2\tau^0 b$, and $b$is the width's structure.

3. The Extraction of Governing Equation

The Hamilton principle is used to obtain the governing vibrational equations (Tauchert, 1974):

$$\int_0^t \delta(U - T - V)dt = 0 \tag{8}$$

where U, T and, Vrepresent the work done by the external forces, kinetic energy, and strain energy, respectively. The strain energy variation for the nanobeam is as follows:

$$\delta U = \int_0^L \left(N\left(\frac{\partial w}{\partial x}\frac{\partial \delta w}{\partial x}\right) - M\delta\left(\frac{\partial^2 w}{\partial x^2}\right)\right) dx \tag{9}$$

In Eq. (9), M and $N$are defined as follows:

$$M = \int_A z t_{xx} dA + \frac{hb}{2} t_{xx}^{s(upper)} - \frac{hb}{2} t_{xx}^{s(lower)} + \int_{\frac{-h}{2}}^{\frac{h}{2}} t_{xx}^{s(left)}\, z dz + \int_{\frac{-h}{2}}^{\frac{h}{2}} t_{xx}^{s(right)}\, z dz \tag{10}$$

$$N = \int_A t_{xx} dA + b\, t_{xx}^{s(upper)} + b t_{xx}^{s(lower)} + \int_{\frac{-h}{2}}^{\frac{h}{2}} t_{xx}^{s(left)}\, dz + \int_{\frac{-h}{2}}^{\frac{h}{2}} t_{xx}^{s(right)}\, dz \tag{11}$$

The kinetic energy variation for the nanobeam is as follows:

$$\int_0^t \delta T\, dt = \rho A \int_0^t \int_0^L \left(\frac{\partial w}{\partial t}\delta\frac{\partial w}{\partial t}\right) dx\, dt = -\rho A \int_0^t \int_0^L \left(\frac{\partial^2 w}{\partial t^2}\delta w\right) dx\, dt \tag{12}$$

The variation of work done by the external forces for the nanobeam is as follows:

$$\delta W = \int_0^L \left(q\delta w + p\frac{\partial w}{\partial x}\delta\frac{\partial w}{\partial x}\right) dx \tag{13}$$

where $q$is defined as:

$$H\frac{\partial^2 w}{\partial x^2} \tag{14}$$

in which the parameter$H$depends on the surface effects defined in Eq. (7). Also, $P$is the magnitude of the compressive pre-load force. By substituting Eqs. (9), (12), and (13) in the Hamilton principle, and by the partial integration of the governing equations on the nanobeam's vibrations, the following is obtained:

$$\frac{\partial N}{\partial x} = 0 \tag{15}$$

$$\frac{\partial^2 M}{\partial x^2} + N\frac{\partial^2 w}{\partial x^2} - p\frac{\partial^2 w}{\partial x^2} + q(x,t) = \rho A\frac{\partial^2 w}{\partial t^2} \tag{16}$$

The boundary condition is obtained as follows:

$$N\frac{\partial w}{\partial x} + \frac{\partial M}{\partial x} - p\frac{\partial w}{\partial x} = 0 or w = 0 \tag{17}$$

$$M = 0 or \frac{\partial w}{\partial x} = 0 \tag{18}$$

Using Eqs. (10) and (11), the force and bending resultants are obtained as follows:

$$N = A_{xx}\frac{1}{2}\left(\frac{\partial w}{\partial x}\right)^2 + B_{xx}\left(\frac{\partial^2 w}{\partial x^2}\right)^2 + C_{xx}\frac{1}{4}\left(\frac{\partial w}{\partial x}\right)^4 \tag{19}$$

$$M = -F_{xx}\frac{\partial^2 w}{\partial x^2} - B_{xx}\left(\frac{\partial w}{\partial x}\right)^2\frac{\partial^2 w}{\partial x^2} \tag{20}$$

In Eqs. (19) and (20), A_{xx}, B_{xx}, C_{xx}, and F_{xx} are defined as follows:

$$\begin{aligned} A_{xx} &= 2E_s(b+h) + Ebh \\ B_{xx} &= 2D^s\left(\frac{bh^2}{4} + \frac{h^3}{12}\right) + D\frac{bh^3}{12} \\ C_{xx} &= 2D^s(b+h) + Dbh \\ F_{xx} &= \left(2E_s\frac{bh^2}{4} + 2E_s\frac{h^3}{12} + E\frac{bh^3}{12}\right) \end{aligned} \tag{21}$$

According to Eq. (15), the force resultant in Eq. (19) is written as:

$$N = \int_0^L \left(A_{xx}\frac{1}{2}\left(\frac{\partial w}{\partial x}\right)^2 + B_{xx}\left(\frac{\partial^2 w}{\partial x^2}\right)^2 + C_{xx}\frac{1}{4}\left(\frac{\partial w}{\partial x}\right)^4\right)dx \tag{22}$$

By placing Eqs. (14) and (20) in Eq. (16), the desirable transverse free nonlinear vibrations of the nanobeam are obtained by considering the nonlinear behavior of surface effects and geometric and material nonlinearities as follows:

$$\left(F_{xx} + B_{xx}\left(\frac{\partial w}{\partial x}\right)^2\right)\frac{\partial^4 w}{\partial x^4} + 2B_{xx}\left(\frac{\partial^2 w}{\partial x^2}\right)^3 + \left(p - N + 6B_{xx}\frac{\partial w}{\partial x}\frac{\partial^3 w}{\partial x^3}\right)\frac{\partial^2 w}{\partial x^2} - H\frac{\partial^2 w}{\partial x^2} + \rho A\frac{\partial^2 w}{\partial t^2} = 0 \tag{23}$$

in which N is based on Eq. (22). Eq. (23) is the governing equation on the transverse free vibrations of nanobeam in the presence of materially nonlinear behaviors for the bulk and surface layers along with nonlinear strains. Coefficients $B_{xx}$and C_{xx} in Eq. (21) show the materially nonlinear of the bulk and materially nonlinear of surface layers, respectively. The solution of Eq. (23) is considered as: $w(x,t) = W(t)\phi(x)$; where $\phi(x)$ for the clamped-clamped boundary condition is defined as follows:

$$\phi(x) = sin\left(\frac{n\pi x}{L}\right) \tag{24}$$

Applying the Galerkin's method to Eq. (23), the following nonlinear differential equation is obtained:

$$\ddot{W} + \omega_{n0}^2 W + \varepsilon_1 W^3 + \varepsilon W^5 = 0 \tag{25}$$

The coefficients of Equation (25) are defined as follows:

$$\begin{aligned} \omega_{n0}^2 &= \frac{(F_{xx}L^2n^4\pi^4 + (H-p)L^4n^2\pi^2)}{\rho AL^6} \\ \varepsilon_1 &= \frac{n^4\pi^4(L^4A_{xx} + 3L^2n^2\pi^2B_{xx})}{4\rho AL^8} \\ \varepsilon &= \frac{3n^6\pi^6C_{xx}L^2}{32\rho AL^8} \end{aligned} \tag{26}$$

In Eq. (25), ω_{n0} stands for the linear frequency of the corresponding system and the fifth-order nonlinearity coefficient in the differential equation coming from the material nonlinearity of the bulk and the nonlinearity of the

surface effects. To solve the nonlinear differential Eq. (25), the modified Lindstedt–Poincaré method will be used, and finally, the results will be validated with the fourth-order Runge-Kutta method. The differential Eq. (25) can be stated as:

$$\ddot{W} + \omega_{nd0}^2 W + \varepsilon\left(\frac{\varepsilon_1}{\varepsilon}W^3 + W^5\right) = 0 \tag{27}$$

in which $f(W)$ can be expressed as:

$$f(W) = \left(\frac{\varepsilon_1}{\varepsilon}W^3 + W^5\right) \tag{28}$$

Assuming $\tau = \omega t$ and $W = a\cos\tau$, where a is the amplitude of the initial condition in the free vibrations, Eq. (28) is rewritten as:

$$f(W) = \frac{\varepsilon_1}{\varepsilon}a^3\cos^3\tau + a^5\cos^5\tau = C_1\cos\tau + C_3\cos 3\tau + C_5\cos 5\tau \tag{29}$$

The nanobeam's nonlinear frequency ω, in the modified Lindstedt–Poincaré method, is extended as (Cheung et al., 1991):

$$\omega^2 = (\omega_{nd0}^2 + \varepsilon\omega_1)\left[1 + \frac{1}{\omega_{nd0}^2 + \varepsilon\omega_1}(\varepsilon^2\omega_2 + \varepsilon^3\omega_3 + \cdots)\right] \tag{30}$$

In the modified Lindstedt–Poincaré method, a new parameter, which is between zero and one, is defined as (Burton, 1984):

$$\alpha = \frac{\varepsilon}{a}\frac{C_H}{\omega_{n0}^2 + \frac{\varepsilon}{a}C_1} \tag{31}$$

In Eq. (31), C_H and other coefficients are defined as:

$$C_H = C_3 + \frac{1}{3}C_5 + \frac{1}{6}C_7 + \cdots$$
$$C_1 = \frac{5a^5}{8} + \frac{3a^3\varepsilon_1}{4\varepsilon}, C_3 = \frac{5a^5}{16} + \frac{a^3\varepsilon_1}{4\varepsilon}, C_5 = \frac{1}{16}a^5 \tag{32}$$

By defining the new parameterα, the expansion of ω^2can be written as:

$$\omega^2 = \omega_{n0}^2\left(1 + \frac{\alpha a\omega_1}{C_H - \alpha C_1}\right)[1 + \delta_2\alpha^2 + \delta_3\alpha^3 + \cdots] \tag{33}$$

In the above equation, δ_i for $i = 2,3,\cdots$ are the unknown coefficients, which will be achieved in the solution process. In the modified Lindstedt–Poincaré method, the solution can be defined as:

$$W = \sum_0^n \alpha^n W_n \tag{34}$$

By changing the variable $\tau = \omega t$and considering $\frac{d^2W}{dt^2} = \omega^2\frac{d^2W}{d\tau^2}$, Eq. (27) is rewritten as:

$$\omega^2 W'' + \omega_{nd0}^2 W + \varepsilon\left(\frac{\varepsilon_1}{\varepsilon}W^3 + W^5\right) = 0 \tag{35}$$

By placing the term ω^2 in Eq. (35), the following equation is obtained:

$$\omega_{nd0}^2\left(1 + \frac{\alpha a\omega_1}{C_H - \alpha C_1}\right)[1 + \delta_2\alpha^2 + \delta_3\alpha^3 + \cdots]W'' + \omega_{n0}^2 W + \frac{\alpha a\omega_{n0}^2}{C_H - \alpha C_1}\left(\frac{\varepsilon_1}{\varepsilon}W^3 + W^5\right) = 0 \tag{36}$$

By simplifying Eq. (36), the following equation is obtained:

$$(C_H - \alpha C_1 + \alpha a\omega_1)[1 + \delta_2\alpha^2 + \delta_3\alpha^3 + \cdots]W'' + (C_H - \alpha C_1)W + \alpha a\left(\frac{\varepsilon_1}{\varepsilon}W^3 + W^5\right) = 0 \tag{37}$$

By placing Eq. (34) in Eq. (37), the following equation is extracted:

$$\begin{gathered}(C_H - \alpha C_1 + \alpha a\omega_1)[1 + \delta_2\alpha^2 + \delta_3\alpha^3 + \delta_4\alpha^4 + \delta_5\alpha^5 + \delta_6\alpha^6] \times \\ \left(W_0'' + \alpha W_1'' + \alpha^2 W_2'' + \alpha^3 W_3'' + \alpha^4 W_4'' + \alpha^5 W_5''\right) + \\ (C_H - \alpha C_1)(W_0 + \alpha W_1 + \alpha^2 W_2 + \alpha^3 W_3 + \alpha^4 W_4 + \alpha^5 W_5) + \\ \alpha a\left[\frac{\varepsilon_1}{\varepsilon}(W_0 + \alpha W_1 + \alpha^2 W_2 + \alpha^3 W_3 + \alpha^4 W_4 + \alpha^5 W_5)^3\right] + \\ \alpha a[(W_0 + \alpha W_1 + \alpha^2 W_2 + \alpha^3 W_3 + \alpha^4 W_4 + \alpha^5 W_5)^5] + \cdots = 0\end{gathered} \tag{38}$$

By simplifying Eq. (38) and rearranging the equation as coefficients of powers α and setting them to zero, the following equations are obtained:

$$\alpha^0: W_0'' + W_0 = 0$$
$$\alpha^1: W_1'' + W_1 = \frac{C_1}{C_H}W_0 + \left(\frac{C_1}{C_H} - \frac{a\omega_1}{C_H}\right)W_0'' - \frac{a\varepsilon_1}{C_H\varepsilon}W_0^3 - \frac{a}{C_H}W_0^5$$
$$\alpha^2: W_2'' + W_2 = \frac{C_1}{C_H}W_1 + \left(\frac{C_1}{C_H} - \frac{a\omega_1}{C_H}\right)W_1'' - \delta_2 W_0'' - \frac{3a\varepsilon_1}{C_H\varepsilon}W_0^2W_1 - \frac{5a}{C_H}W_0^4W_1$$
$$\alpha^3: W_3'' + W_3 = \frac{C_1}{C_H}W_2 + \left(\frac{C_1\delta_2}{C_H} - \delta_3 - \frac{a\delta_2\omega_1}{C_H}\right)W_2'' - \delta_2 W_1'' + \left(\frac{C_1}{C_H} - \frac{a\omega_1}{C_H}\right)W_2'' - \frac{3a\varepsilon_1}{C_H\varepsilon}W_1^2W_0 - \frac{3a\varepsilon_1}{C_H\varepsilon}W_0^2W_1 - \frac{5a}{C_H}W_0^4W_2 - \frac{10a}{C_H}W_0^3W_1^2 \quad (39)$$

The solution of the equation containing α^0 with assumed initial conditions as $W_0(0) = a$ and $W_0'(0) = 0$ is achievable as:

$$W_0 = a\cos\tau \quad (40)$$

Substituting W_0 in the equation in which α^1 exists leads to the following equation:

$$W_1'' + W_1 = \frac{C_1}{C_H}W_0 + \left(\frac{C_1}{C_H} - \frac{a\omega_1}{C_H}\right)W_0'' - \frac{a\varepsilon_1}{C_H\varepsilon}W_0^3 - \frac{a}{C_H}W_0^5$$
$$= \left(-\frac{5a^6}{8C_H} - \frac{3a^4\varepsilon_1}{4C_H\varepsilon} + \frac{a^2\omega_1}{C_H}\right)\cos\tau + \left(-\frac{5a^6}{16C_H} - \frac{a^4\varepsilon_1}{4C_H\varepsilon}\right)\cos(3\tau) - \frac{a^6}{16C_H}\cos(5\tau) \quad (41)$$

In the differential Eq. (41), the coefficient of the term$\cos\tau$is the secular term whose value must be equal to zero, so ω_1 can be expressed as:

$$\omega_1 = \frac{a^2}{8\varepsilon}(5a^2\varepsilon + 6\varepsilon_1) \quad (42)$$

The solution of the Eq. (41) is obtained by considering the initial conditions $W_1(0) = 0$ and $W_1'(0) = 0$as follows:

$$W_1 = \left(-\frac{a^6}{24C_H} - \frac{a^4\varepsilon_1}{32C_H\varepsilon}\right)\cos\tau + \left(\frac{5a^6}{128C_H} + \frac{a^4\varepsilon_1}{32C_H\varepsilon}\right)\cos(3\tau) + \frac{a^6}{384C_H}\cos(5\tau) \quad (43)$$

By placing the solution W_1 and W_0 in the equation, including the coefficient α^2, the following equation can be obtained:

$$W_2'' + W_2 = \left(\frac{35a^{11}}{512{C_H}^2} + a\delta_2 + \frac{29a^9\varepsilon_1}{256{C_H}^2\varepsilon} + \frac{3a^7{\varepsilon_1}^2}{64{C_H}^2\varepsilon^2} - \frac{a^7\omega_1}{24{C_H}^2} - \frac{a^5\varepsilon_1\omega_1}{32{C_H}^2\varepsilon}\right)\cos\tau$$
$$+\left(-\frac{35a^{11}}{3072{C_H}^2} - \frac{5a^6C_1}{16{C_H}^2} - \frac{5a^9\varepsilon_1}{128{C_H}^2\varepsilon} - \frac{a^4C_1\varepsilon_1}{4{C_H}^2\varepsilon} - \frac{3a^7{\varepsilon_1}^2}{128{C_H}^2\varepsilon^2} + \frac{45a^7\omega_1}{128{C_H}^2} + \frac{9a^5\varepsilon_1\omega_1}{32{C_H}^2\varepsilon}\right)\cos(3\tau)$$
$$+\left(-\frac{125a^{11}}{3072{C_H}^2} - \frac{a^6C_1}{16{C_H}^2} - \frac{a^9\varepsilon_1}{16{C_H}^2\varepsilon} - \frac{3a^7{\varepsilon_1}^2}{128{C_H}^2\varepsilon^2} + \frac{25a^7\omega_1}{384{C_H}^2}\right)\cos(5\tau)$$
$$+\left(-\frac{95a^{11}}{6144{C_H}^2} - \frac{3a^9\varepsilon_1}{256{C_H}^2\varepsilon}\right)\cos(7\tau) - \frac{5a^{11}}{6144{C_H}^2}\cos(9\tau) \quad (44)$$

In the Eq. (44), by setting $\cos\tau$to zero, δ_2 will be as follows:

$$\delta_2 = -\frac{a^4(105a^6\varepsilon^2 + 174a^4\varepsilon\varepsilon_1 + 72a^2{\varepsilon_1}^2 - 64a^2\varepsilon^2\omega_1 - 48\varepsilon\varepsilon_1\omega_1)}{1536{C_H}^2\varepsilon^2} \quad (45)$$

By placing ω_1 in Eq. (45), δ_2 is simplified as:

$$\delta_2 = -\frac{a^6(65a^4\varepsilon^2 + 96a^2\varepsilon\varepsilon_1 + 36{\varepsilon_1}^2)}{1536C_H^2\varepsilon^2} \quad (46)$$

Finally, the solution of the differential equation, including α^2 and by consideration of the initial conditions $W_2(0) = 0$ and $W_2'(0) = 0$, and replacing $\omega_1$and δ_2, can be achieved as:

$$W_2 = \left(-\frac{509a^{11}}{147456{C_H}^2} - \frac{a^6C_1}{24{C_H}^2} - \frac{95a^9\varepsilon_1}{12288{C_H}^2\varepsilon} - \frac{a^4C_1\varepsilon_1}{32{C_H}^2\varepsilon} - \frac{a^7{\varepsilon_1}^2}{256{C_H}^2\varepsilon^2} + \frac{215a^7\omega_1}{4608{C_H}^2} + \frac{9a^5\varepsilon_1\omega_1}{256{C_H}^2\varepsilon}\right)\cos\tau$$
$$+\left(\frac{35a^{11}}{24576{C_H}^2} + \frac{5a^6C_1}{128{C_H}^2} + \frac{5a^9\varepsilon_1}{1024{C_H}^2\varepsilon} + \frac{a^4C_1\varepsilon_1}{32{C_H}^2\varepsilon} + \frac{3a^7{\varepsilon_1}^2}{1024{C_H}^2\varepsilon^2} - \frac{45a^7\omega_1}{1024{C_H}^2} - \frac{9a^5\varepsilon_1\omega_1}{256{C_H}^2\varepsilon}\right)\cos(3\tau)$$
$$+\left(\frac{125a^{11}}{73728{C_H}^2} + \frac{a^6C_1}{384{C_H}^2} + \frac{a^9\varepsilon_1}{384{C_H}^2\varepsilon} + \frac{a^7{\varepsilon_1}^2}{1024{C_H}^2\varepsilon^2} - \frac{25a^7\omega_1}{9216{C_H}^2}\right)\cos(5\tau)$$

$$+\left(\frac{95a^{11}}{294912{C_H}^2}+\frac{a^9\varepsilon_1}{4096{C_H}^2\varepsilon}\right)cos(7\tau)+\frac{a^{11}}{98304{C_H}^2}cos(9\tau) \quad (47)$$

By obtaining $W_1$and W_2, the final solution will be as:

$$W = W_0 + \alpha W_1 + \alpha^2 W_2 \quad (48)$$

By placing $W_1$and W_2 in the final solution, Wwill be achieved as:

$$W=\left[a+\alpha\left(-\frac{a^6}{24C_H}-\frac{a^4\varepsilon_1}{32C_H\varepsilon}\right)+\alpha^2\left(-\frac{509a^{11}}{147456{C_H}^2}-\frac{a^6C_1}{24{C_H}^2}-\frac{95a^9\varepsilon_1}{12288{C_H}^2\varepsilon}-\frac{a^4C_1\varepsilon_1}{32{C_H}^2\varepsilon}-\frac{a^7{\varepsilon_1}^2}{256{C_H}^2\varepsilon^2}+\frac{215a^7\omega_1}{4608{C_H}^2}+\frac{9a^5\varepsilon_1\omega_1}{256{C_H}^2\varepsilon}\right)\right]cos\,\tau$$
$$+\left[\alpha\left(\frac{5a^6}{128C_H}+\frac{a^4\varepsilon_1}{32C_H\varepsilon}\right)+\alpha^2\left(\frac{35a^{11}}{24576{C_H}^2}+\frac{5a^6C_1}{128{C_H}^2}+\frac{5a^9\varepsilon_1}{1024{C_H}^2\varepsilon}+\frac{a^4C_1\varepsilon_1}{32{C_H}^2\varepsilon}+\frac{3a^7{\varepsilon_1}^2}{1024{C_H}^2\varepsilon^2}-\frac{45a^7\omega_1}{1024{C_H}^2}-\frac{9a^5\varepsilon_1\omega_1}{256{C_H}^2\varepsilon}\right)\right]cos(3\tau)$$
$$+\left[\alpha\frac{a^6}{384C_H}+\alpha^2\left(\frac{125a^{11}}{73728{C_H}^2}+\frac{a^6C_1}{384{C_H}^2}+\frac{a^9\varepsilon_1}{384{C_H}^2\varepsilon}+\frac{a^7{\varepsilon_1}^2}{1024{C_H}^2\varepsilon^2}-\frac{25a^7\omega_1}{9216{C_H}^2}\right)\right]cos(5\tau)+\alpha^2\left[\frac{95a^{11}}{294912{C_H}^2}+\frac{a^9\varepsilon_1}{4096{C_H}^2\varepsilon}\right]cos(7\tau)+\alpha^2\frac{a^{11}}{98304{C_H}^2}cos(9\tau) \quad (49)$$

Eventually, by solving the two of terms of the modified Lindstedt–Poincaré method, the dimensionless nonlinear frequency of the nanobeam can be written as:

$$\omega=\sqrt{\omega_{n0}^2\left(1+\frac{\alpha\frac{a^3}{8\varepsilon}(5a^2\varepsilon+6\varepsilon_1)}{C_H-\alpha C_1}\right)} \quad (50)$$

Also, the nonlinear non-dimensional frequency of the nanobeam for the three terms of the modified Lindstedt–Poincaré method of the solution is as follows:

$$\omega=\sqrt{\omega_{n0}^2\left(1+\frac{\alpha\frac{a^3}{8\varepsilon}(5a^2\varepsilon+6\varepsilon_1)}{C_H-\alpha C_1}\right)\left[1+\left(-\frac{a^6(65a^4\varepsilon^2+96a^2\varepsilon\varepsilon_1+36{\varepsilon_1}^2)}{1536C_H^2\varepsilon^2}\right)\alpha^2\right]} \quad (51)$$

4. Results Status

In this section, the results obtained from the modified Lindstedt–Poincaré method are examined by considering the materially nonlinear behavior of the bulk and surface effects for nanobeam which is shown in Fig1. Furthermore, the nonlinear frequency and free response of the nanobeam are investigated in the presence of material and geometric nonlinearities. In the results, the volumetric mass and Young's modulus of the nanobeam are considered $2300\frac{kg}{m^3}$and $1TPa$, respectively. Table 1 shows the comparison between the nanobeam's nonlinear frequency ratio and previous studies. In this table, the dimensionless natural frequency is as follows:

$$\text{Nonlinear frequency ratio}=\frac{\text{Nonlinear natural frequency}}{\text{Linear natural frequency}} \quad (52)$$

Also, in this table, the material nonlinear parameters and the longitudinal scale are zero. As can be seen, the results obtained in the table below are consistent with the previous researches.

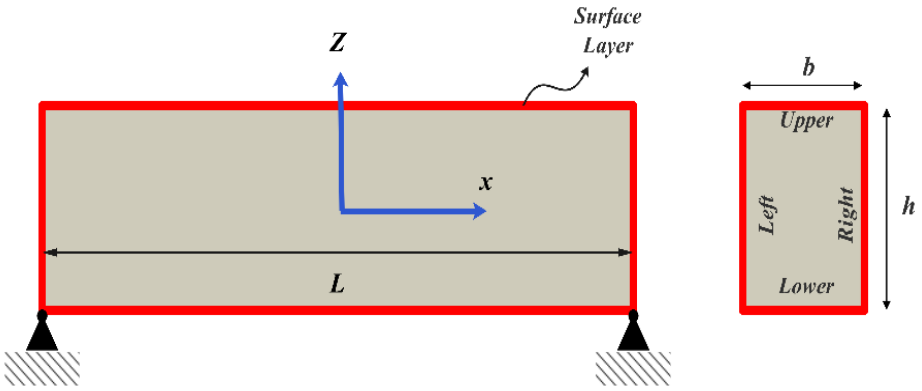

Figure 1: Schematic of Nanobeam

Table 1: The Comparison of Nonlinear Frequency's Ratio of the Nanobeam for *L=2, h=0.1* (Nazemnezhad & Hosseini-Hashemi, 2014).

A(nm)	Present	Ref. (Singh et al., 1990)	Ref. (Nageswara Rao, 1992)	Ref. (Nazemnezhad & Hosseini-Hashemi, 2014)
$\frac{h}{\sqrt{12}}$	1.08916	1.0892	1.0889	1.0937
$\frac{2h}{\sqrt{12}}$	1.31776	1.3178	1.3183	1.3750
$\frac{3h}{\sqrt{12}}$	1.62561	1.6257	1.6260	1.8438

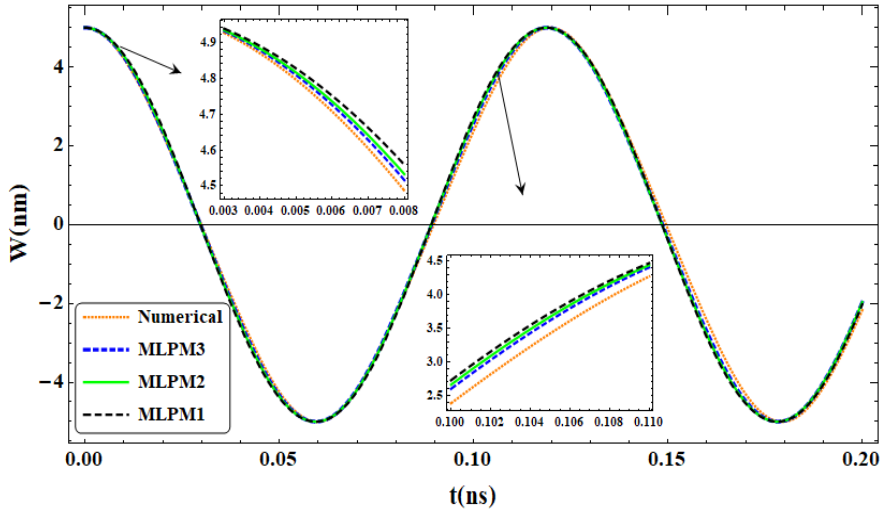

Figure 2: The Convergence of the Nanobeam's Response Obtained from the Modified Lindstedt–Poincaré Method by Numerical Solution for $L = 100nm, h = a = 5nm, b = 2h, D = -2TPa, D^s = -50\frac{N}{m}, E_s = 6\frac{N}{m}, \tau^0 = 3\frac{N}{m}, p = 10nN$.

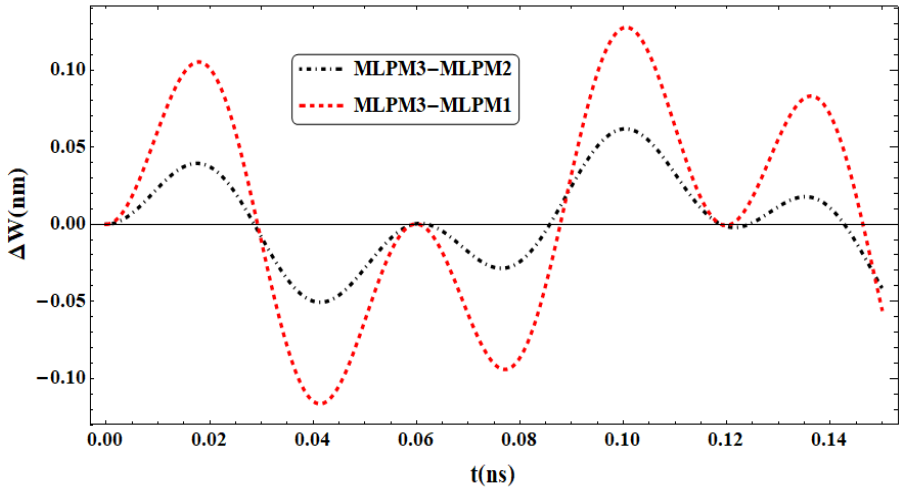

Figure 3: The Difference Between Obtained Responses by Considering One, Two, and Three Terms of the Modified Lindstedt–Poincaré Method for $L = 100nm, h = a = 5nm, b = 2h, D = -2TPa, D^s = -50\frac{N}{m}, E_s = 6\frac{N}{m}, \tau^0 = 3\frac{N}{m}, p = 10nN$.

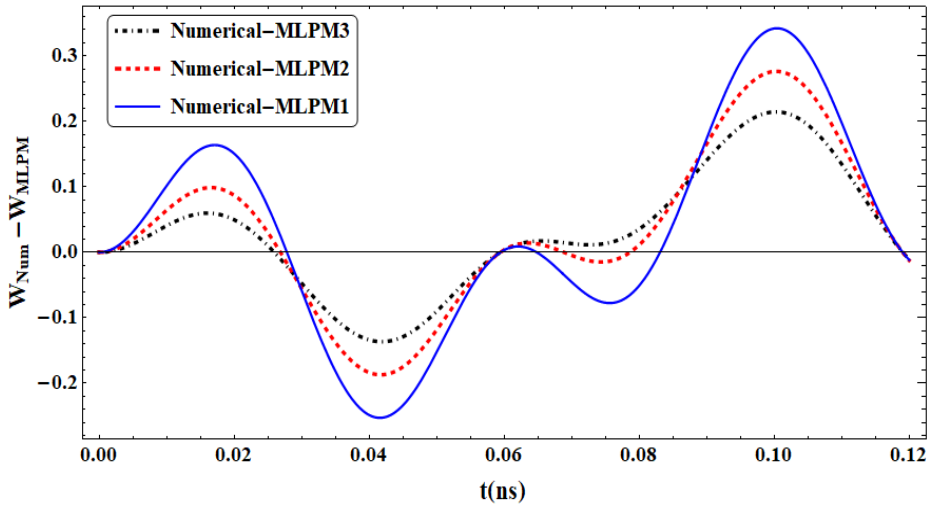

Figure 4: The Difference Between the Modified Lindstedt–Poincaré Method and the Fourth-Order Runge–Kutta Numerical Solution for $L = 100nm, h = a = 5nm, b = 2h, D = -2TPa, D^s = -50\frac{N}{m}, E_s = 6\frac{N}{m}, \tau^0 = 3\frac{N}{m}, p = 10nN$

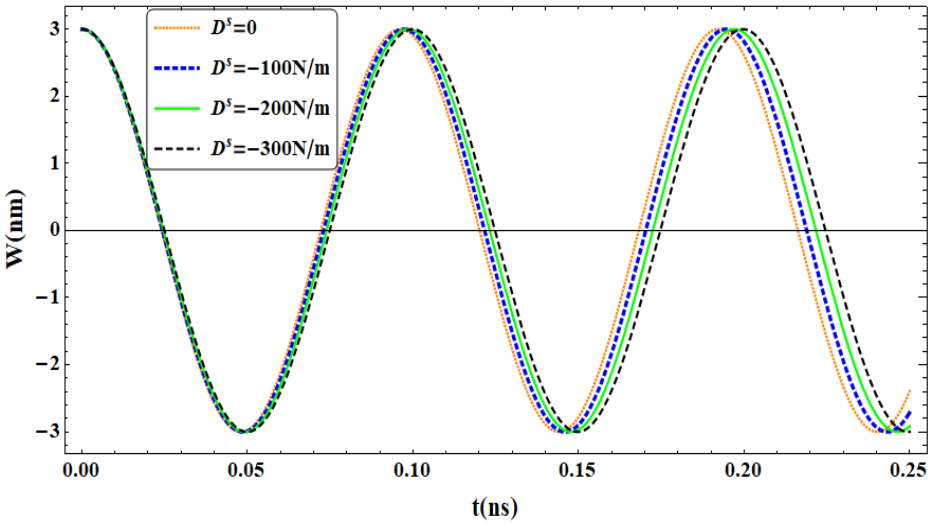

Figure 5: The nanobeam's Response for Different Values of Third-Order Elastic Modulus D^s and $L = 20nm, h = a = 3nm, b = 2h, D = -2TPa, E_s = 6\frac{N}{m}, \tau^0 = 3\frac{N}{m}, p = 10nN$.

Figure 2 illustrates the convergence of the nanobeam's response obtained from the modified Lindstedt–Poincaré method by a numerical solution of the fourth-order Runge-Kutta. In this figure, $MLPM1$,$MLPM2$, and$MLPM3$ represent the one, two, and three terms of the Lindstedt–Poincaré method. As can be seen, increasing the terms of the modified Lindstedt–Poincaré solution leads to the convergence of the nanobeam's response to the numerical solution. Figure 3 depicts the difference in the dimensionless responses for one, two, and three terms of the modified Lindstedt–Poincaré method. The difference in the solution at the extremum points of the graph in the case $MLPM3 - MLPM1$ is greater than the case $MLPM3 - MLPM2$. Figure 4 demonstrates the difference between responses obtained from the Lindstedt–Poincaré method and numerical solution. The difference between the modified Lindstedt–Poincaré method by considering three terms ($MLPM3$) and numerical solution is less than the other two cases. In other words, increasing the number of terms of the modified Lindstedt–Poincaré method reduces the error compared to the numerical solution. Figure 5 shows the nanobeam's dimensionless response for different values of the third-order surface modulus of elasticity. This parameter causes material nonlinearity in surface effects. Therefore, in this figure, rising the size of the surface's third-order elastic modulus increases the nanobeam's time period, and this causes the extremum of the dimensionless response to shift.

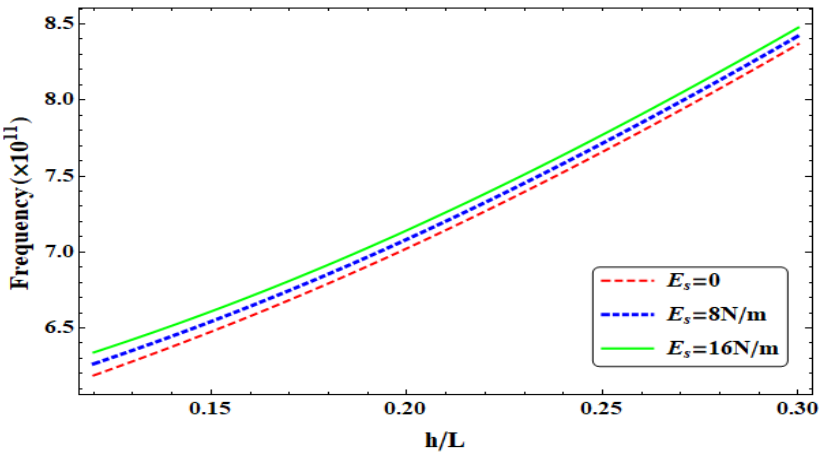

Figure 6: Nonlinear Frequency for Different Values of Surface Elastic Modulus Versus Thickness-to-Length Ratio $L = 20nm, h = a = 4nm, b = 2h, D = -2TPa, D^s = -150\frac{N}{m}, \tau^0 = 3\frac{N}{m}, p = 10nN$.

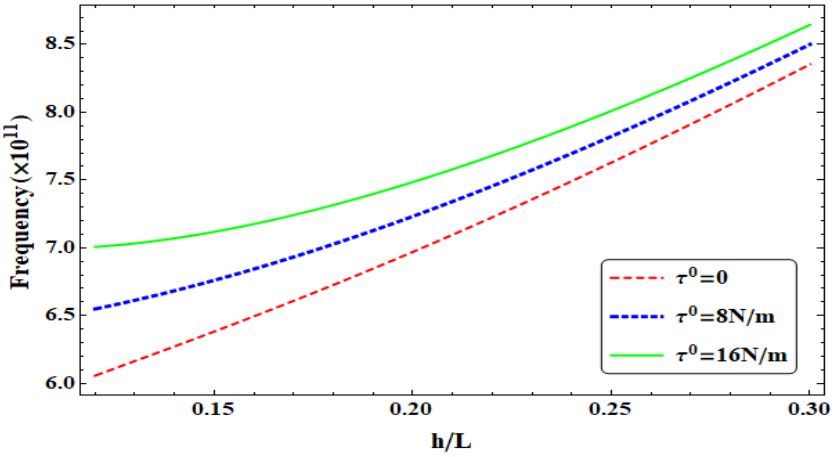

Figure 7: Nonlinear Frequency for Different Values of the Residual Surface Tension Versus Thickness-to-Length Ratio $L = 20nm, h = a = 4nm, b = 2h, D = -2TPa, D^s = -150\frac{N}{m}, E_s = 3\frac{N}{m}, p = 10nN$.

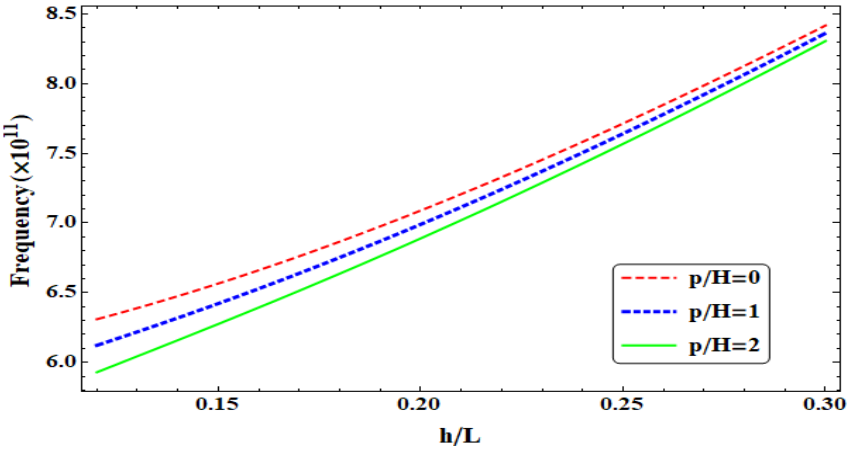

Figure 8: Nonlinear frequency for different values of the dimensionless compressive pre-load versus thickness-to-length ratio $L = 20nm, h = a = 4nm, b = 2h, D = -2TPa, D^s = -150\frac{N}{m}, E_s = 3\frac{N}{m}, \tau^0 = 3\frac{N}{m}$.

Figure 6 shows the nonlinear frequency of the nanobeam for different values of surface elastic modulus versus thickness-to-length ratio. Increasing the thickness-to-length ratio increases the stiffness of the nanobeam, and thus it increases the nonlinear frequency of the nanobeam. Also, in this figure, increasing the surface elastic modulus increases the stiffness of the nanobeam, which raise the nonlinear frequency of the nanobeam. Figure 7 illustrates the nonlinear frequency of nanobeam for different amounts of residual surface tension versus thickness-to-length ratio. It is obvious that the increase in the residual surface tension increases the stiffness of the nanobeam, and then it increases the nonlinear frequency of the nanobeam. From Figures 6 and 7, raising the residual surface tension has led to more changes in the nonlinear frequency diagram than the increase in surface elastic modulus. Figure 8 demonstrates the nonlinear frequency of the nanobeam for different amounts of dimensionless compressive pre-load force $\frac{p}{H}$against thickness-to-length ratio. In this figure, increasing the compressive pre-load force reduces the nonlinear frequency of the nanobeam.

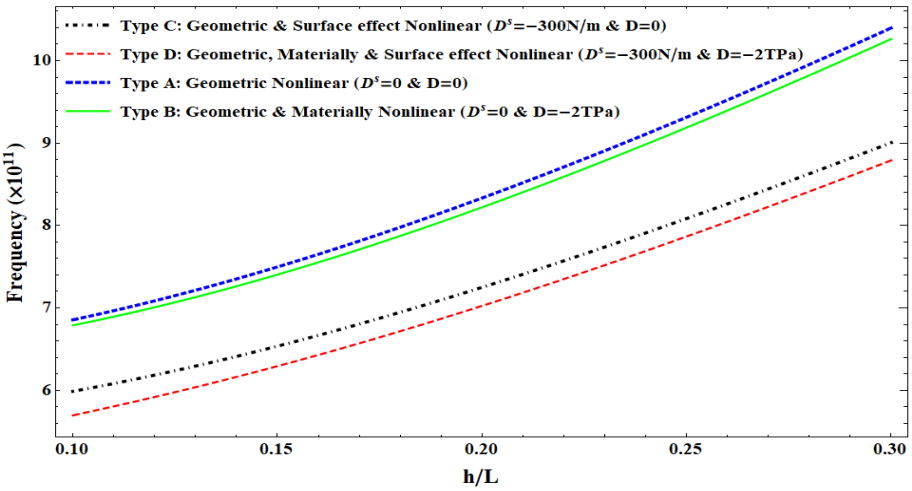

Figure 9: The Nonlinear Frequency of the Nanobeam for Different Nonlinearities Versus Thickness-to-Length Ratio.

Figure 9 depicts the nanobeam's nonlinear frequency for material nonlinearity of bulk D and materially nonlinear of surface layers D^s and geometric nonlinearity due to Von Kármán strains. As can be seen in this figure, there is a geometric nonlinearity for all states. The first state-considering the geometric nonlinearity and linear behaviors of the bulk and surface layers (Type A), the nonlinear frequency of the nanobeam is higher than other types which are shown in this figure. The second state-the presence of either nonlinearity (Type B and Type C) along with geometric nonlinearity causes the nonlinear frequency of the nanobeam to decrease in comparison with the first case because the coefficients of the third-order elastic modulus $D$and third-order surface elastic modulus D^spossess negative signs. Therefore, these coefficients reduce the strain energy of the nanobeam and consequently reduce the nonlinear frequency of the nanobeam, and the amount of this reduction depends on the amounts of D and D^s. The third state-the simultaneous presence of nonlinearities (Type D) along with geometric nonlinearity causes the nonlinear frequency to decrease more than all types because $D$and D^scause further decreases in the strain energy. Consequently, leads to a further decrease in the nonlinear frequency than in the previous two states.

5. Conclusion

In this paper, free vibrations of the nanobeam are investigated by considering the materially nonlinear behaviors of bulk and surface layers. The results of this study indicate the following:

- The free-response obtained from the modified Lindstedt–Poincaré method was converged by growing the number of solution's terms to the numerical solution of the fourth-order of Runge-Kutta in the presence of the materially nonlinear bulk and materially nonlinear surface layers.
- Increasing the dimensionless compressive force declined the nonlinear frequency of the nanobeam.
- The difference between the solution obtained from the modified Lindstedt–Poincaré method and the numerical solution for three terms of the solution is less than the one and two terms coming from the modified Lindstedt–Poincaré incare method.
- Increasing the size of the third-order surface modulus increases the free response of the period.

- Reducing the residual surface tension reduces the nonlinear frequency of the nanobeam.
- Increasing the third-order elastic modulus and the third-order surface modulus of elasticity increase and decrease the nonlinear frequency of the nanobeam, respectively.
- The simultaneous effect of material nonlinearities of the bulk and surface layers cause a large reduction in the nanobeam nonlinear frequency compared to the other cases.

References

Alam, M., & Mishra, S. K. (2021). Nonlinear vibration of nonlocal strain gradient functionally graded beam on nonlinear compliant substrate. *Composite Structures*, *263*, 113447. https://doi.org/10.1016/j.compstruct.2020.113447

Alizadeh Hamidi, B., Khosravi, F., Hosseini, S. A., & Hassannejad, R. (2020). Closed form solution for dynamic analysis of rectangular nanorod based on nonlocal strain gradient. *Waves in Random and Complex Media*, 1-17. https://doi.org/10.1080/17455030.2020.1843737

Arash, B., & Wang, Q. (2013). Detection of gas atoms with carbon nanotubes. *Scientific reports*, *3*(1), 1-6. https://doi.org/10.1038/srep01782

Bunch, J. S., Van Der Zande, A. M., Verbridge, S. S., Frank, I. W., Tanenbaum, D. M., Parpia, J. M., Craighead, H. G., & McEuen, P. L. (2007). Electromechanical resonators from graphene sheets. *science*, *315*(5811), 490-493. https://doi.org/10.1126/science.1136836

Burton, T. (1984). A perturbation method for certain non-linear oscillators. *International Journal of Non-Linear Mechanics*, *19*(5), 397-407. https://doi.org/10.1016/0020-7462(84)90026-X

Cammarata, R. C. (1994). Surface and interface stress effects in thin films. *Progress in surface science*, *46*(1), 1-38. https://doi.org/10.1016/0079-6816(94)90005-1

Chen, C., Shi, Y., Zhang, Y. S., Zhu, J., & Yan, Y. (2006). Size dependence of Young's modulus in ZnO nanowires. *Physical review letters*, *96*(7), 075505. https://doi.org/10.1103/PhysRevLett.96.075505

Chen, T., Chiu, M.-S., & Weng, C.-N. (2006). Derivation of the generalized Young-Laplace equation of curved interfaces in nanoscaled solids. *Journal of Applied Physics*, *100*(7), 074308. https://doi.org/10.1063/1.2356094

Cheung, Y., Chen, S., & Lau, S. (1991). A modified Lindstedt-Poincaré method for certain strongly non-linear oscillators. *International Journal of Non-Linear Mechanics*, *26*(3-4), 367-378. https://doi.org/10.1016/0020-7462(91)90066-3

Dang, V.-H. (2020). Buckling and nonlinear vibration of size-dependent nanobeam based on the non-local strain gradient theory. *Journal of Applied Nonlinear Dynamics*, *9*(3), 427-446. https://doi.org/10.5890/JAND.2020.09.007

Dang, V. H., & Nguyen, T. H. (2021). Buckling and nonlinear vibration of functionally graded porous micro-beam resting on elastic foundation. *Mechanics of Advanced Composite Structures*. https://doi.org/10.22075/macs.2021.24098.1350

Ebrahimi, F., & Hosseini, S. H. S. (2021). Nonlinear vibration and dynamic instability analysis nanobeams under thermo-magneto-mechanical loads: a parametric excitation study. *Engineering with Computers*, *37*(1), 395-408. https://doi.org/10.1007/s00366-019-00830-0

Esfahani, S., Khadem, S. E., & Mamaghani, A. E. (2019). Nonlinear vibration analysis of an electrostatic functionally graded nano-resonator with surface effects based on nonlocal strain gradient theory. *International Journal of Mechanical Sciences*, *151*, 508-522. https://doi.org/10.1016/j.ijmecsci.2018.11.030

Gheshlaghi, B., & Hasheminejad, S. M. (2011). Surface effects on nonlinear free vibration of nanobeams. *Composites Part B: Engineering*, *42*(4), 934-937. https://doi.org/10.1016/j.compositesb.2010.12.026

Gurtin, M., Weissmüller, J., & Larche, F. (1998). A general theory of curved deformable interfaces in solids at equilibrium. *Philosophical Magazine A*, *78*(5), 1093-1109. https://doi.org/10.1080/01418619808239977

Hamidi, B. A., Hosseini, S. A., Hassannejad, R., & Khosravi, F. (2020). Theoretical analysis of thermoelastic damping of silver nanobeam resonators based on Green–Naghdi via nonlocal elasticity with surface energy effects. *The European Physical Journal Plus*, *135*(1), 1-20. https://doi.org/10.1140/epjp/s13360-019-00037-8

Hamidi, B. A., Hosseini, S. A., Hayati, H., & Hassannejad, R. (2020). Forced axial vibration of micro and nanobeam

under axial harmonic moving and constant distributed forces via nonlocal strain gradient theory. *Mechanics Based Design of Structures and Machines*, 1-15. https://doi.org/10.1080/15397734.2020.1744003

Hieu, D.-V., & Bui, G.-P. (2020). Nonlinear vibration of a functionally graded nanobeam based on the nonlocal strain gradient theory considering thickness effect. *Advances in Civil Engineering*, *2020*. https://doi.org/10.1155/2020/9407673

Jazi, S. H. (2020). Nonlinear vibration of an elastically connected double Timoshenko nanobeam system carrying a moving particle based on modified couple stress theory. *Archive of Applied Mechanics*, *90*(12), 2739-2754. https://doi.org/10.1007/s00419-020-01746-8

Kakei, A., Epaarachchi, J., Islam, M., & Leng, J. (2018). Evaluation of delamination crack tip in woven fibre glass reinforced polymer composite using FBG sensor spectra and thermo-elastic response. *Measurement*, *122*, 178-185. https://doi.org/10.1016/j.measurement.2018.03.023

Kakei, A., Manuela, J., Srinivasan, V., Sharda, A., Islam, M., & Epaarachchi, J. (2019). Investigation of FBG sensor performance in detection of delamination damage in a half-conical shape composite component. In *Proceedings of the 12th International Workshop on Structural Health Monitoring* (Vol. 2, pp. 2973-2979). https://doi.org/10.12783/shm2019/32451

Khosravi, F., Hosseini, S. A., & Hamidi, B. A. (2020). Torsional Vibration of nanowire with equilateral triangle cross section based on nonlocal strain gradient for various boundary conditions: comparison with hollow elliptical cross section. *The European Physical Journal Plus*, *135*(3), 1-20. https://doi.org/10.1140/epjp/s13360-020-00312-z

Khosravi, F., Hosseini, S. A., Hamidi, B. A., Dimitri, R., & Tornabene, F. (2020). Nonlocal torsional vibration of elliptical nanorods with different boundary conditions. *Vibration*, *3*(3), 189-203. https://doi.org/10.3390/vibration3030015

Kuilla, T., Bhadra, S., Yao, D., Kim, N. H., Bose, S., & Lee, J. H. (2010). Recent advances in graphene based polymer composites. *Progress in polymer science*, *35*(11), 1350-1375. https://doi.org/10.1016/j.progpolymsci.2010.07.005

Lee, C., Wei, X., Kysar, J. W., & Hone, J. (2008). Measurement of the elastic properties and intrinsic strength of monolayer graphene. *science*, *321*(5887), 385-388. https://doi.org/10.1126/science.1157996

Mahmoud, M. A. (2016). Validity and accuracy of resonance shift prediction formulas for microcantilevers: a review and comparative study. *Critical Reviews in Solid State and Materials Sciences*, *41*(5), 386-429. https://doi.org/10.1080/10408436.2016.1142858

Nageswara Rao, B. (1992). Large-amplitude free vibrations of simply supported uniform beams with immovable ends. *Journal of Sound Vibration*, *155*(3), 523-527. https://ui.adsabs.harvard.edu/abs/1992JSV...155..523N/abstract

Nazemnezhad, R., & Hosseini-Hashemi, S. (2014). Nonlocal nonlinear free vibration of functionally graded nanobeams. *Composite Structures*, *110*, 192-199. https://doi.org/10.1016/j.compstruct.2013.12.006

Nejad, M. Z., Hadi, A., & Rastgoo, A. (2016). Buckling analysis of arbitrary two-directional functionally graded Euler–Bernoulli nano-beams based on nonlocal elasticity theory. *International Journal of Engineering Science*, *103*, 1-10. https://doi.org/10.1016/j.ijengsci.2016.03.001

Noroozi, M., & Ghadiri, M. (2020). Nonlinear vibration and stability analysis of a size-dependent viscoelastic cantilever nanobeam with axial excitation. *Proceedings of the Institution of Mechanical Engineers, Part C: Journal of Mechanical Engineering Science*, 0954406220959104. https://doi.org/10.1177/0954406220959104

Qasim, B. M., Khidir, T. C., Hameed, A. F., & Abduljabbar, A. A. (2018). Influence of heat treatment on the absorbed energy of carbon steel alloys using oil quenching and water quenching. *Journal of Mechanical Engineering Research and Developments*, *41*(3), 43-46. https://doi.org/10.26480/jmerd.03.2018.43.46

Rao, S. S. (2007). *Vibration of continuous systems* (Vol. 464). Wiley Online Library. https://wp.kntu.ac.ir/hrahmanei/Adv-Vibrations-Books/Continuous-Vibrations-Rao.pdf

Shafiei, N., Kazemi, M., Safi, M., & Ghadiri, M. (2016). Nonlinear vibration of axially functionally graded non-uniform nanobeams. *International Journal of Engineering Science*, *106*, 77-94. https://doi.org/10.1016/j.ijengsci.2016.05.009

Şimşek, M. (2014). Large amplitude free vibration of nanobeams with various boundary conditions based on the

nonlocal elasticity theory. *Composites Part B: Engineering*, *56*, 621-628. https://doi.org/10.1016/j.compositesb.2013.08.082

Singh, G., Rao, G. V., & Iyengar, N. (1990). Re-investigation of large-amplitude free vibrations of beams using finite elements. *Journal of Sound and Vibration*, *143*(2), 351-355. https://doi.org/10.1016/0022-460X(90)90958-3

Sourani, P., Hashemian, M., Pirmoradian, M., & Toghraie, D. (2020). A comparison of the Bolotin and incremental harmonic balance methods in the dynamic stability analysis of an Euler–Bernoulli nanobeam based on the nonlocal strain gradient theory and surface effects. *Mechanics of Materials*, *145*, 103403. https://doi.org/10.1016/j.mechmat.2020.103403

Tauchert, T. R. (1974). *Energy principles in structural mechanics*. McGraw-Hill Companies. https://cir.nii.ac.jp/crid/1130282271700195968

Wang, G.-F., & Feng, X.-Q. (2007). Effects of surface elasticity and residual surface tension on the natural frequency of microbeams. *Applied physics letters*, *90*(23), 231904. https://doi.org/10.1063/1.2746950

Wang, G.-F., & Feng, X.-Q. (2009). Surface effects on buckling of nanowires under uniaxial compression. *Applied physics letters*, *94*(14), 141913. https://doi.org/10.1063/1.3117505

Wang, K., & Wang, B. (2011). Vibration of nanoscale plates with surface energy via nonlocal elasticity. *Physica E: Low-dimensional Systems and Nanostructures*, *44*(2), 448-453. https://doi.org/10.1016/j.physe.2011.09.019

Zhao, D., Wang, J., & Xu, Z. (2021). Surface Effect on Vibration of Timoshenko Nanobeam Based on Generalized Differential Quadrature Method and Molecular Dynamics Simulation. *Nanomanufacturing and Metrology*, *4*(4), 298-313. https://doi.org/10.1007/s41871-021-00117-3

Zhao, K., Pharr, M., Hartle, L., Vlassak, J. J., & Suo, Z. (2012). Fracture and debonding in lithium-ion batteries with electrodes of hollow core–shell nanostructures. *Journal of Power Sources*, *218*, 6-14. https://doi.org/10.1016/j.jpowsour.2012.06.074